

# Finite element analysis of the temperature dependent conductivity of metallic hollow sphere structures

**T. Fiedler, A. Öchsner**

Department of Mechanical Engineering,  
Centre for Mechanical Technology and Automation,  
University of Aveiro, 3810-193 Aveiro, Portugal  
tfiedler, aoechsner@mec.ua.pt

## ABSTRACT

In the scope of this study, finite element analysis is applied in order to determine the effective thermal conductivity of periodic metallic hollow sphere structures (MHSS). Two different joining technologies for the connection of the hollow spheres, namely sintering and adhesive bonding, are considered. For the determination of the thermal conductivity of the MHSS, the temperature dependence of the thermal conductivities of the base materials, i.e. hollow spheres and joining element, are considered. Two different cases, a low and a high temperature gradient within the structure are distinguished. Furthermore, the overall thermal conductivities of sandwich panels with an insulating MHSS core in dependence on the relative face sheet thickness are investigated.

Keywords: thermal conductivity; hollow sphere structure; non-linear analysis; sandwich panel

## 1. INTRODUCTION

Hollow sphere structures (cf. Fig. 1) constitute an innovative group of advanced composite materials. Their characteristics comprise high specific stiffness, good damping properties, energy absorption and thermal insulation (e.g. [1,2]). Combination of these

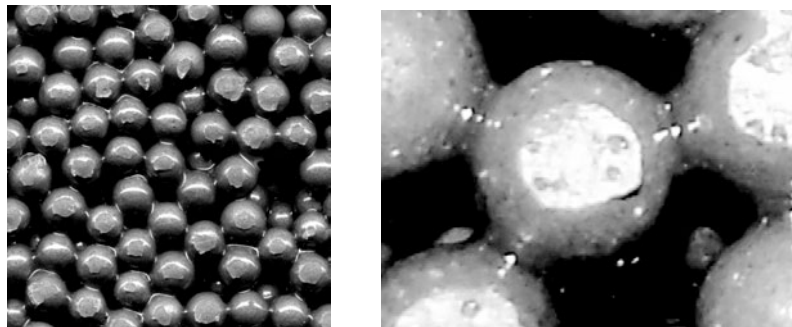


Figure 1 Adhesively bonded hollow sphere structures.

properties opens a wide field of potential multifunctional applications e.g. in automotive or aerospace industry.

Hollow sphere structures are assembled by single metallic hollow spheres. The coherence of the hollow spheres can be achieved by different joining technologies such as sintering and adhesion. Consequently, the thermal characteristics of the structure depend on the geometry of the structure and thermal properties of the base materials. The high volume fraction of the closed porosity of the structure in combination with a low thermal conductivity of the epoxy resin suggests the application of such materials for thermal insulation.

## 2. FINITE ELEMENT APPROACH

The analysis of the thermal conductivity is performed by means of a finite element approach. The finite element model of the microstructure is illustrated in Fig. 2, where the light grey elements correspond to the metallic sphere, whereas the dark grey elements are related to the joint. Depending on the considered joining technology, the joint represents the sintered neck or the adhesive connection between two neighbouring spheres. Corresponding to measurements *on specimens*, the outer diameter  $R$  of the hollow spheres is 1 mm, the sphere wall thickness  $d$  is 0.033 mm and the minimum distance between two neighbouring spheres  $a_{\min}$  is 0.06 mm.

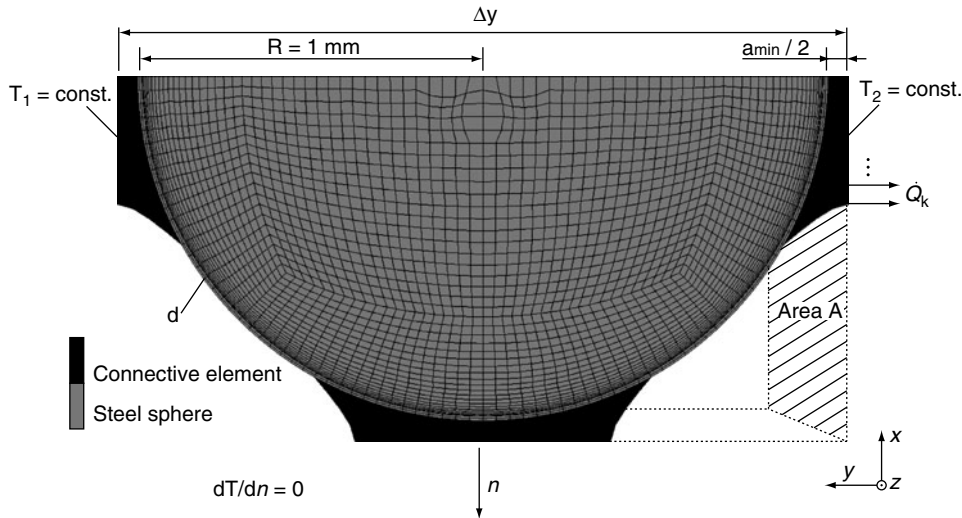


Figure 2 Finite element model of the unit cell of a hollow sphere structure.

At the left and right side of the joints two constant temperatures  $T_1$  and  $T_2$  are prescribed. The nodal heat flux in the direction perpendicular to these surfaces is notated as  $\dot{Q}_k(T_1, T_2)$ . The total heat flux through one of the surfaces is given by

$$\dot{Q}(T_1, T_2) = \sum_k \dot{Q}_k(T_1, T_2). \quad (1)$$

The heat flux perpendicular to all remaining surfaces is zero which corresponds to periodic boundary conditions.

It is shown in [3,4] that the influence of thermal radiation on the effective thermal conductivity of porous metals, especially at temperatures below 700K is low and can therefore be disregarded. Furthermore, the open porosity of MHSS is small and consequently also the effect of convection is excluded from the numerical simulation. Due to these simplifications, Fourier's law yields the effective thermal conductivity  $\lambda(T_1, T_2)$  of the structure:

$$\lambda(T_1, T_2) = \frac{\dot{Q}(T_1, T_2)}{A} \cdot \frac{\Delta y}{\Delta T} \quad (2)$$

The specific distance  $\Delta y = 2.12$  mm and the projected area  $A = 1.06^2$  mm<sup>2</sup> are defined by the geometry, the temperature difference  $\Delta T = T_2 - T_1$  is given by the boundary conditions and the total heat flux  $\dot{Q}_k(T_1, T_2)$  is result of the finite element calculation.

In a second step of the finite element analysis, the results of the thermal conductivities of the microstructure (unit cell) at low temperature gradients are assigned to a homogenised finite element model. Therefore, a simple mesh is assembled by planar rectangular elements (thickness 1) with the thermal conductivity corresponding to the results obtained for the microstructure. This procedure allows for the simulation of large MHSS without the necessity of modelling the whole microstructure consisting of numerous cells. Two Al UNS96061 face sheets are added to the homogenised finite element model of the core in order to generate a sandwich structure with a varying face sheet thickness  $t$ . The evaluation of the thermal conductivity of the sandwich structure is performed according to eqn (2).

The thermal conductivities  $\lambda$  of the base material in dependence on the temperature  $T$  are illustrated in Fig. 3. It can be seen that the thermal conductivity of the metals Al UNS96061 [5] and Ck67 [6] distinctly exceed the values of the epoxy resin Hysol FP4401 [7].

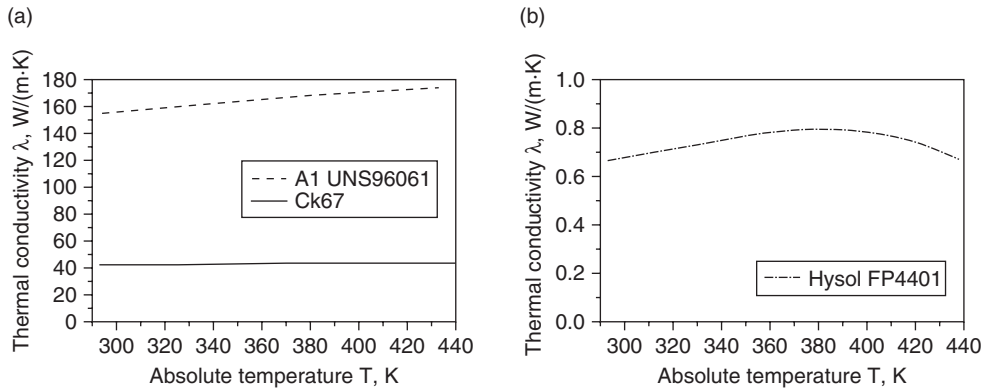


Figure 3 Thermal conductivities of the base materials in dependence on the absolute temperature.

### 3. EFFECTIVE THERMAL CONDUCTIVITY

The determination of the effective thermal conductivity of MHSS requires the distinction of two different cases. First, a low temperature gradient where the temperature is approximately constant within one unit cell and second a high temperature gradient, where the changing temperature dependence of the base materials of the structure has to be accounted for inside the unit cell.

### 3.1. LOW TEMPERATURE GRADIENT

In the case of a low temperature gradient, the temperature inside one unit cell can be regarded as approximately constant. Therefore, the thermal conductivity of the MHSS can be determined only in dependence on this temperature. The temperature boundary conditions (cf. Fig. 2) are  $T_1 = T_i - 0.01\text{K}$  and  $T_2 = T_i + 0.01\text{K}$  for  $T_i = 293, 303, \dots, 433\text{K}$  and the results of these calculations are summarised in Fig. 4.

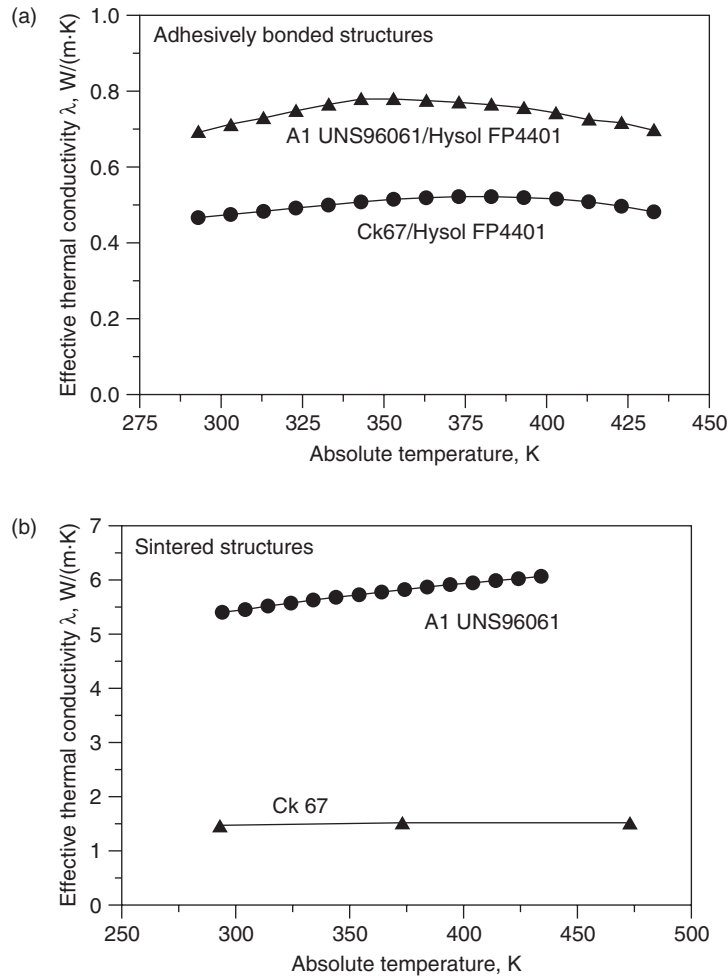


Figure 4 Thermal conductivities of unit cells with low temperature gradients in dependence on the absolute temperature.

Fig. 4a visualises the temperature dependence of the thermal conductivity of adhesively bonded MHSS. In comparison to the results of sintered structures (cf. Fig. 4b), the values of adhesively bonded MHSS are lower. The adhesively bonded structures exhibits a maximum of the conductivity at approximately 340K (Al/Hysol), respectively 390K (Ck67/Hysol). The conductivity of the sintered structures linearly rises with the absolute temperature within the regarded range. The high thermal conductivity of the aluminium alloy (cf. Fig. 3) also

increases the thermal conductivity of MHSS. In comparison, the utilisation of CK67 as sphere wall material decreases the thermal conductivity of the structure.

### 3.2. HIGH TEMPERATURE GRADIENT

In contrast to the simplification in the previous section, high temperature gradients require the consideration of the temperature distribution inside the unit cell. Due to the temperature dependence of the thermal conductivities of the base materials (cf. Fig. 3), the thermal conductivity of the unit cell depends on the absolute values of both temperatures  $T_1$  and  $T_2$  and can therefore not be determined for particular temperatures.

In order to confine the complexity of this investigation, the temperature  $T_1$  is fixed at the constant temperature 298K (approximately room temperature) and only the temperature  $T_2$  is varied between 323, 348, ..., 423K (glass transition temperature 433K [8] of the considered epoxy resin). The results are obtained for the unit cell as well as for a homogenised model of the MHSS. The homogenised model is assembled by planar rectangular elements and exhibits the thermal properties obtained in the previous section for the MHSS and low temperature gradients.

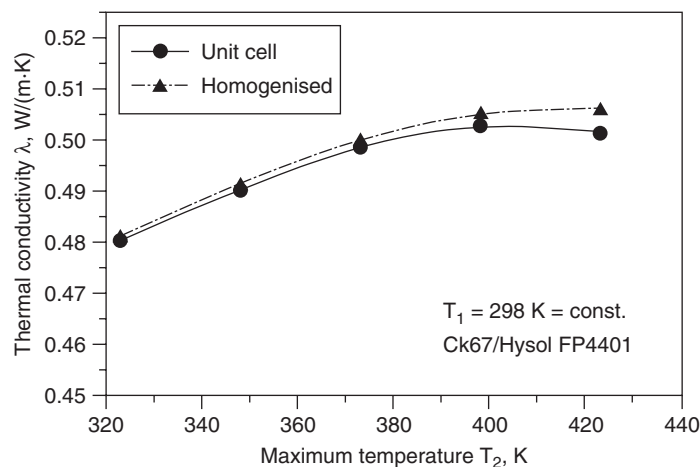


Figure 5 Comparison of the thermal conductivities of unit cells and homogenised models with differing temperature gradients.

Figure 5 visualises the results of both analyses. In the case of low temperature gradients (e.g.  $\Delta T/\Delta y = 25\text{K}/2.12\text{ mm}$ ) the results obtained for both models almost coincide. However, also for the maximum temperature difference of 125K the deviation reaches only 0.93%.

### 3.3. SANDWICH STRUCTURE

In the following, sandwich panels with MHSS cores acting as a thermal insulating layer are considered. The effective thermal conductivity is determined in the direction of the normal vector of the face sheets. The temperatures prescribed at the upper and lower surfaces are 293K and 433K, respectively. The microstructure of the MHSS is homogenised and therefore represented by plane rectangular elements in order to reduce the required calculation time. As shown in the previous section, the deviation introduced by this simplification is small.

Figure 6 summarises the results of this investigation. The effective thermal conductivity  $\lambda$  is plotted versus the normalised face sheet thickness. This ratio is equal to the varying thickness  $t$  of the face sheets divided by the constant total height  $h = 30$  mm of the structure and is defined for values between 0 (pure core material) and 0.5 (no core material, face sheets merge).

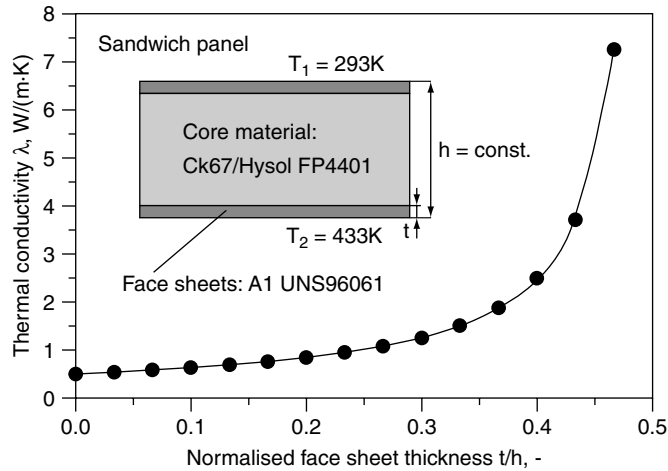


Figure 6 Thermal conductivity of sandwich panels with HSS-cores in dependence on the normalised face sheet thickness.

The thermal conductivity of the sandwich structure increases with increasing relative thickness of the face sheets. This phenomenon can be explained with the high thermal conductivity of aluminium alloy (cf. Fig. 3) in comparison to the insulating MHSS core material. Even in the case of very thin insulating layers ( $t/h = 0.4$ ) the thermal conductivity of the sandwich panel only reaches ca. 1.5% of the values of the face sheet material. However, for further decrease of the thickness of the core, the thermal conductivity of the structure grows exponentially.

Next, the adhesive layers joining face sheets and core material are incorporated in the numerical simulation. The overall height  $h$  of the structure is 30 mm and the face sheet thickness  $t$  is 1 mm. Two different adhesive interface layers with a thickness  $t_{\text{Adh}}$  of 0.25 and 0.5 mm are considered. These interface layers exhibit the thermal properties of Hysol FP4401 (cf. Fig. 3b) which is multiplied by a scale factor  $s = 0.8, 1.0, 1.2$  in order to account for a change of the material properties due to chemical reactions. The findings are shown in Table 1.

Table 1 Thermal conductivities of sandwich structures ( $t = 2$  mm) with adhesive interface layers

	Scale factor $s$			Without interface layer
	0.8	1	1.2	
$t_{\text{Adh}} = 0.25$ mm	0.582 W / (m · K)	0.584 W / (m · K)	0.585 W / (m · K)	0.581 W / (m · K)
$t_{\text{Adh}} = 0.5$ mm	0.583 W / (m · K)	0.587 W / (m · K)	0.590 W / (m · K)	

It can be seen that the influence of the interface layer on the overall thermal conductivity is low. This result can be explained by the similar thermal conductivities of the adhesively bonded hollow sphere structure (cf. Fig. 4a) and the adhesive (cf. Fig. 3b). The influence slightly increases with growing thickness  $t_{\text{Adh}}$  of the adhesive interface layer.

#### 4. CONCLUSIONS

In this paper, the effective thermal conductivity of MHSS is numerically determined. Thereby, the temperature dependence of the thermal conductivities of the base materials is considered. First, the case of low temperature gradients is investigated, where the temperature inside one unit cell (microstructure, cf. Fig. 2) is approximately constant. It is found that the results obtained for the microstructure and low temperature gradients can be applied in homogenised models also for high temperature gradients. Comparison of these results with simulations performed on the microstructure at high temperature gradients exhibits a good approximation. This allows the numerical simulation of the thermal behaviour of MHSS at low computational costs. Furthermore, the effectiveness of MHSS as thermal insulating layer inside sandwich panels is demonstrated. A critical value of ca. 0.4 is identified, where the thermal conductivity rises exponentially for further increase of the normalised face sheet thickness. An adhesive thermal interface layer shows no significant influence on the thermal overall conductivity of the sandwich structure.

#### REFERENCES

- [1] Degischer, H., Kriszt, B., *Handbook of Cellular Metals*, Wiley-VCH, Weinheim, 2002.
- [2] Ashby, M.F., Evans, A., Flech, N.A., Gibson, L.J., Hutchinson, J.W. and Wadley, H.N.G., *Metal Foams — A Design Guide*, Butterworth-Heinemann, Woburn 2000.
- [3] Lu, T.J., Thermal Transport and Fire Retardance Properties of Cellular Aluminium Alloys, *Acta Materialia*, 1999, 47, pp. 1469–1485.
- [4] Öchsner, A., Grácio, J., On the macroscopic thermal properties of syntactic metal foams., *Multidiscipline Modelling in Materials and Structures*, 2005, 1, pp. 171–181.
- [5] NIST Cryogenic Technologies Group, Bolder CO, *Military-Handbook-5H*, 1998, pp. 3–261.
- [6] MSC.Marc, Material Database.
- [7] Nyilas, A., Rehme, R., Wyrwich, C., Springer, H. and Hinrichsen, G., Thermal diffusivity and conductivity of highly filled epoxies as cover materials for microelectronic devices as measured by the heat pulse technique, *Journal of Materials Science Letters*, 1996, 15, p. 1457.
- [8] Technical Data Sheet, Loctite®.

#### ACKNOWLEDGEMENTS

The authors are grateful to Portuguese Foundation of Science and Technology for financial support.

